

# A Map of the Distal Region of the Long Arm of Human Chromosome 21 Constructed by Radiation Hybrid Mapping and Pulsed-Field Gel Electrophoresis

MARGIT BURMEISTER,<sup>\*</sup>1 SUWON KIM,† E. ROYDON PRICE,†,2 TITIA DE LANGE,§,3 UMADEVI TANTRAVAHU,||,4 RICHARD M. MYERS,<sup>\*</sup>‡ AND DAVID R. COX†,‡

Departments of <sup>\*</sup>Physiology, †Psychiatry, ‡Biochemistry and Biophysics, and §Microbiology and Immunology, University of California, San Francisco, California 94143; and ||Genetics Division, Children's Hospital, Harvard University School of Medicine, Boston, Massachusetts 02115

Received June 6, 1990; revised August 28, 1990

We have used radiation hybrid (RH) mapping and pulsed-field gel electrophoresis (PFGE) to determine the order and positions of 28 DNA markers from the distal region of the long arm of human chromosome 21. The maps generated by these two methods are in good agreement. This study, combined with that of D. R. Cox *et al.* (1990, *Science* 250:245-250), results in an RH map that covers the long arm of chromosome 21 (21q). We have used a subtelomeric probe to show that our map includes the telomere and have identified single-copy genes and markers within 200 kbp of the telomere. Comparison of the physical and RH maps with genetic linkage maps shows "hot spots" of meiotic recombination in the distal region, one of which is close to the telomere, in agreement with previous cytogenetic observations of increased recombination frequency near telomeres.

© 1991 Academic Press, Inc.

## INTRODUCTION

In the past 10 years, a major effort in molecular genetics has been made in generating maps of genomes. A breakthrough in human gene mapping was the development of DNA markers for linkage analysis, which has resulted in near completion of a genetic map of the human genome at a resolution of about 10-20 cM (e.g., Donis-Keller *et al.*, 1987). The genetic map has been useful for mapping human disease genes to chromosomal regions, but a much higher res-

olution map is needed for cloning genes and for genome organization studies. High-resolution maps cannot be constructed easily by meiotic linkage methods because their resolution is low at the molecular level, recombination frequency is not linearly correlated with physical distance, and only the subset of markers that recognizes polymorphisms can be mapped.

The development of pulsed-field gel electrophoresis (PFGE, Schwartz and Cantor, 1984) allows the generation of physical maps several megabase pairs in size (for example, Burmeister *et al.*, 1988; Fulton *et al.*, 1989). However, PFGE is not easily applied to the construction of maps of whole chromosomes. With the very large number of probes necessary to create such large maps, DNA probes often recognize fragments of the same size by coincidence. Therefore, an additional method that could be used in conjunction with PFGE to determine the order of markers would be useful.

Somatic cell hybrids containing defined segments of a chromosome of interest can provide information about the order of probes along the chromosome. However, the resolution of maps constructed with such cell lines is usually limited by the small number of available hybrids. In an effort to obtain maps of higher resolution, we have developed a somatic cell hybrid mapping strategy called radiation hybrid (RH) mapping (Cox *et al.*, 1990). In this procedure, a hybrid cell line containing a single human chromosome in a rodent cell background is subjected to a high dose of X-rays, which results in chromosomal fragmentation. The chromosomal fragments are recovered by fusion to a rodent recipient cell line, which nonselectively retains some hamster and human chromosomal pieces from the donor cell line. DNA markers near one another on the chromosome are likely to be re-

<sup>1</sup> To whom correspondence should be addressed at Department of Physiology, S-762, University of California Medical School, 513 Parnassus Avenue, San Francisco CA 94143-0444.

<sup>2</sup> Present address: Department of Genetics, 25 Shattuck Avenue, Harvard University School of Medicine, Boston, MA 02115.

<sup>3</sup> Present address: Rockefeller University, New York, NY 10021.

<sup>4</sup> Present address: Department of Obstetrics and Gynecology, Columbia University, New York, NY 10032.

tained or lost together in any particular hybrid cell line. Although many cell lines contain several non-contiguous pieces of DNA from the human chromosome, it is nevertheless possible to use a statistical analysis of cosegregation of markers to construct a map of higher resolution than is possible by classical somatic cell genetic approaches (Cox *et al.*, 1990).

Chromosome 21, the smallest human chromosome, is a paradigm for large-scale human genome mapping efforts. A high-resolution map of chromosome 21 is of particular interest since trisomy 21 results in Down syndrome, the most frequent cause of mental retardation and birth defects in humans. Several meiotic maps of chromosome 21 have been published recently (Tanzi *et al.*, 1988; Warren *et al.*, 1989; Petersen *et al.*, 1989). Gardiner *et al.* (1988, 1990) analyzed chromosome 21 by using somatic cell hybrids and PFGE. In their physical mapping studies, probes close to one another were linked into clusters, and markers were localized into sections along the chromosome. However, the order of markers within sections and the physical distances between many markers could not be determined. Recently, we combined RH mapping with PFGE to determine the order of 14 markers spanning approximately 20 million base pairs on the proximal long arm of chromosome 21 (Cox *et al.*, 1990). Here we use this combined approach to order 28 markers in the distal region of the long arm of chromosome 21 and to construct a continuous physical map of the most telomeric 8000 kbp of the long arm, including the telomere itself. A comparison of the physical map with the genetic linkage map of this segment of the chromosome reveals several hot spots of meiotic recombination. In addition, the physical map helps to define rearrangements that have occurred in this region of the genome during evolution.

## MATERIALS AND METHODS

### DNA Markers

In this paper we use abbreviations for the locus names determined by the Human Gene Mapping workshops (HGM). For example, S3 represents D21S3, etc. Note, however, that S100B is the gene for the  $\beta$ -subunit of the protein S100 rather than the locus D21S100. Details about the DNA probes used in this study have been described: S3 (pPW231c), S55 (pPW518-1R), and S58 (pPW524-5P) (Watkins *et al.*, 1985); S101 (JG373) (Galt *et al.*, 1989); S15 (pGSE8), S17 (pGSH8), and S19 (pGSB3) (Stewart *et al.*, 1985); S39 (SF13A), S40 (SF14), S41 (SF21), S42 (SF43), S44 (SF50), S49 (SF58), and S51 (SF93) (Korenberg *et al.*, 1987); S123 (B88) and S141 (E73) (Tantravahi *et al.*, 1988); S25 (p10.2) (Millington and

Pearson, 1988); pTH2 $\Delta$  (de Lange *et al.*, 1990); MxA and MxB (Aebi *et al.*, 1989); BCE-I (pS2) (Moisan *et al.*, 1988); PFKL (cPFKL3.0) (Levanon *et al.*, 1987); CD18 (Mac3 and Mac9) (Kishimoto *et al.*, 1987); COL6A1 (cA1) and COL6A2 (cA2) (Weil *et al.*, 1988); SOD1 (pHG-SOD) (Liemman-Hurwitz *et al.*, 1982); S100B (pHS22.4) (Allore *et al.*, 1988). A probe for human  $\alpha$ -crystallin-1 (CRYA1) was obtained by amplifying a 3.5-kbp DNA fragment between exons 1 and 3 from the sequences described (McDevitt *et al.*, 1986) by using the polymerase chain reaction (Saiki *et al.*, 1988). After amplification, ends were repaired with Klenow and T4 polymerase, and the product was subcloned into pUC18.

### Radiation Hybrid Mapping

RH mapping can be used to determine the order and distance between DNA markers by analyzing the presence or absence of such markers in somatic cell hybrids following exposure to X-rays (Cox *et al.*, 1989, 1990). We used the cell line CHG3, a hybrid cell line containing human chromosome 21 in a hamster cell background (a subclone of 72532X-6, Patterson *et al.*, 1985) to construct the RH map in this study exactly as described (Cox *et al.*, 1990). The distance between two markers as determined by RH mapping is expressed in centirays (cR), analogous to centimorgans (cM) in meiotic linkage mapping. Because RH distance depends on the amount of irradiation used to fragment the chromosomes, it is important to include information about X-ray dose when describing the centiray distance between two markers. A distance of 1 cR<sub>8000</sub> between two markers corresponds to a 1% frequency of breakage between the markers after exposure to 8000 rads of X-rays (Cox *et al.*, 1990). Four-point analysis is used to calculate the odds favoring one order of four markers over another order (Cox *et al.*, 1990).

### Pulsed-Field Gel Electrophoresis

We used DNA from the hybrid cell line CHG3 (see above) and from human blood cells to generate physical maps. To avoid problems in interpreting results due to polymorphisms, the blood cell DNA used throughout this study was prepared from a single individual. The methods for preparation of agarose blocks containing high-molecular-weight DNA, preparation of yeast and bacteriophage  $\lambda$  multimers as size markers, restriction digests, alkaline blotting, and subsequent hybridization of GeneScreen membranes were as described (Herrmann *et al.*, 1987). In general,

**TABLE 1**  
**RH Mapping: Analysis of Hybrids and Calculated Distances**

| Marker A | Marker B | No. of clones observed |    |    |    | Total | $\theta$ | cR <sub>8000</sub> | Lod   |
|----------|----------|------------------------|----|----|----|-------|----------|--------------------|-------|
|          |          | ++                     | +- | -+ | -- |       |          |                    |       |
| S40      | S49      | 19                     | 0  | 1  | 30 | 50    | 0.05     | 5                  | 12.82 |
| CD18     | S25      | 7                      | 0  | 1  | 36 | 44    | 0.06     | 7                  | 7.22  |
| S39      | S40      | 21                     | 0  | 2  | 48 | 71    | 0.07     | 7                  | 15.27 |
| S44      | COL6A2   | 15                     | 2  | 0  | 33 | 50    | 0.09     | 10                 | 10.08 |
| S40      | S141     | 16                     | 1  | 1  | 25 | 43    | 0.11     | 11                 | 9.54  |
| S55      | S3       | 15                     | 2  | 1  | 38 | 56    | 0.12     | 13                 | 9.91  |
| S141     | CD18     | 8                      | 0  | 2  | 30 | 40    | 0.13     | 13                 | 6.28  |
| COL6A1   | COL6A2   | 14                     | 3  | 0  | 31 | 48    | 0.14     | 15                 | 8.39  |
| S44      | COL6A1   | 25                     | 2  | 3  | 49 | 79    | 0.14     | 15                 | 14.20 |
| S39      | S49      | 18                     | 1  | 3  | 43 | 65    | 0.15     | 16                 | 11.10 |
| S101     | S39      | 16                     | 3  | 1  | 41 | 61    | 0.16     | 17                 | 9.84  |
| S49      | S141     | 18                     | 3  | 1  | 38 | 60    | 0.15     | 17                 | 10.35 |
| S3       | S101     | 9                      | 3  | 0  | 31 | 43    | 0.17     | 18                 | 6.12  |
| S25      | S44      | 13                     | 0  | 4  | 37 | 54    | 0.18     | 20                 | 8.15  |
| CD18     | S44      | 16                     | 0  | 5  | 47 | 68    | 0.18     | 20                 | 10.19 |
| COL6A1   | S100B    | 21                     | 4  | 2  | 46 | 73    | 0.19     | 21                 | 11.40 |
| SOD1     | S58      | 18                     | 4  | 1  | 31 | 54    | 0.19     | 22                 | 8.44  |
| S49      | CD18     | 8                      | 2  | 2  | 36 | 48    | 0.21     | 23                 | 5.76  |
| S25      | COL6A2   | 4                      | 1  | 1  | 17 | 23    | 0.22     | 25                 | 2.61  |
| COL6A2   | S100B    | 10                     | 3  | 1  | 28 | 42    | 0.23     | 26                 | 5.38  |
| S141     | S25      | 12                     | 4  | 1  | 34 | 51    | 0.25     | 28                 | 6.51  |
| S55      | S101     | 15                     | 4  | 2  | 33 | 54    | 0.25     | 29                 | 6.98  |
| S3       | S39      | 14                     | 6  | 1  | 45 | 66    | 0.26     | 30                 | 7.40  |
| S101     | S40      | 14                     | 3  | 3  | 27 | 47    | 0.30     | 35                 | 5.93  |
| S17      | S55      | 12                     | 5  | 2  | 31 | 50    | 0.31     | 37                 | 5.02  |
| S58      | S17      | 13                     | 3  | 5  | 31 | 52    | 0.34     | 41                 | 4.95  |
| S17      | S3       | 13                     | 6  | 3  | 35 | 57    | 0.36     | 45                 | 4.90  |
| S58      | S55      | 22                     | 9  | 6  | 44 | 81    | 0.40     | 52                 | 6.55  |
| SOD1     | S17      | 13                     | 9  | 6  | 28 | 56    | 0.57     | 84                 | 2.23  |

*Note.* Selected marker pairs, designated Marker A and Marker B, are included. The number of hybrid cell clones analyzed for each marker pair is indicated, with ++ indicating the number of hybrids containing both markers A and B, +- indicating the number of hybrids containing marker A but not marker B, -+ indicating the number of hybrids containing marker B but not marker A, and -- indicating the number of hybrids containing neither marker.  $\theta$  indicates the estimated frequency of X-ray breakage between Markers A and B, and cR<sub>8000</sub> indicates the distance between the two markers (5). Marker pairs with a lod score of 3.0 or greater are considered to be significantly linked. Only these marker pairs are used to construct the RH map (5).

PFGE was performed at 15°C in 0.5× TBE buffer. CHEF gel electrophoresis was performed in a CHEF apparatus constructed at the EMBL (Heidelberg, FRG) according to Chu *et al.* (1986). OFAGE was performed in an apparatus obtained from LKB-Pharmacia.

To test whether two probes hybridize to the same fragment, we always used the same filter. Probes were removed from a filter before hybridization with the next probe by placing the filter into a solution containing 2 mM Tris/HCl, pH 8, 0.2 mM EDTA, 0.1% SDS at 80°C twice for 20 min.

DNA fragments were separated in two ranges of resolution, low resolution (500–3000 kbp) and high resolution (50–900 kbp). Within each range, several sets of filters were prepared. Probes close to each other were compared on identical filters. The prior information from RH mapping and/or genetic map-

ping therefore helped to determine which probes were likely to be physically linked.

## RESULTS

### Mapping Strategy

To generate a map of human chromosome 21 distal to the marker SOD1, we first chose 19 markers as landmarks for radiation hybrid mapping. The RH map constructed from these landmarks was then used as an aid in the physical mapping of the most distal region of human chromosome 21, the region including and distal to the marker D21S3. In addition to this initial set of 19 markers, which was analyzed by both RH mapping and PFGE, we analyzed a set of markers by PFGE only (Table 2). These additional markers were included primarily because they were used as

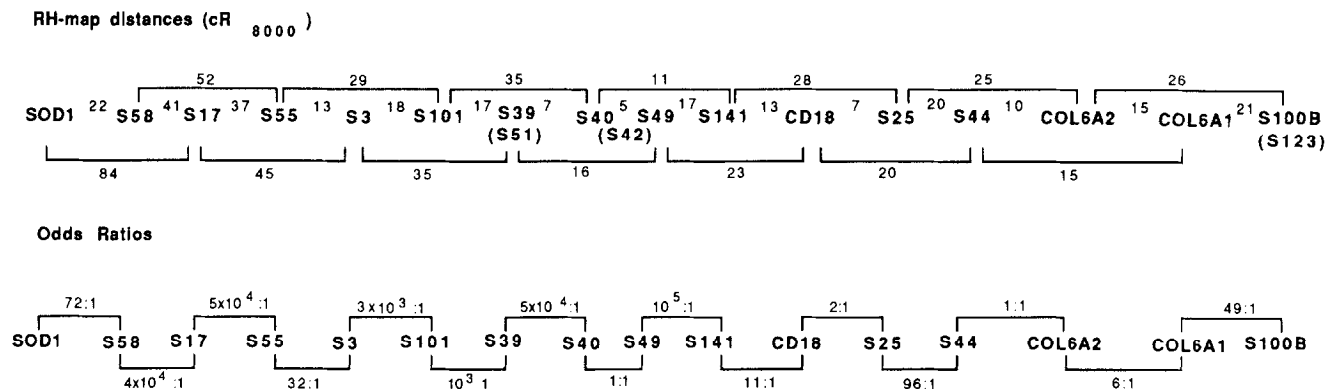


FIG. 1. Radiation hybrid map. The map shows the order of probes, as derived by RH mapping, and the distance between each pair. The telomere is to the right, near S100B. Distances for adjacent markers are shown between the markers, and for nearest neighbor pairs above and below the map. Loci shown in parentheses are those that were not separated by RH mapping from the loci indicated above them, and were not used for the construction of the map. S42 was not separated from either S40 or S49, although these two loci are separated in a cell line for which S42 was not scored. The odds favoring the order indicated compared to the order in which the given marker pair is inverted (5) are shown below the map.

anchor points in recently published genetic maps (Petersen *et al.*, 1989; Tanzi *et al.*, 1988; Warren *et al.*, 1989).

#### Radiation Hybrid Mapping

Our initial set of 19 markers was analyzed by RH mapping (Cox *et al.*, 1990). Cell hybrids containing chromosome 21 fragments generated by X-ray breakage were scored for the presence or absence of these markers. These primary data were analyzed as pairwise combinations of markers by using a computer program that we developed for RH mapping (Cox *et al.*, 1990). Four of the marker pairs, S100B and S123, S51 and S39, S40 and S42, and S42 and S49, were not separated by X-ray breakage in any of the radiation hybrids that were analyzed. For each of these pairs of markers, only the marker scored for the largest number of hybrids was included in the mapping analysis, which included 16 loci. A sample of the most pertinent marker pairs is listed in Table 1. Pairs of markers with a lod score of 3.0 or greater were considered to be significantly linked, and the two-point distances of only linked marker pairs were used to construct a map. We defined the best order of markers as the one in which the sum of the distances between adjacent markers was minimized. This analysis resulted in the map shown in Fig. 1. Four-point analysis (Cox *et al.*, 1990) was used to calculate the relative likelihood of one order of four markers versus another. Each odds ratio shown below the map in Fig. 1 represents the odds of the illustrated order of four markers compared to the order in which the internal two markers are inverted. Some of these odds ratios are less than 1000:1. In these cases, it is not possible to establish marker order with certainty using the RH data alone.

Therefore, pulsed-field gel electrophoresis was used in an effort to obtain a more definitive order.

#### Long-Range Restriction Mapping of the Most Distal 8000 kbp by PFGE

PFGE mapping requires that markers be physically linked on identical large DNA fragments. To cover large distances, fragments in the size range of 200 to 2500 kbp were separated by CHEF electrophoresis, blotted onto membranes, and hybridized successively with the labeled probes. Enzymes resulting in fragment sizes in this range were *NruI*, *MluI*, *SalI*, *NotI*, and, in some cases, *RsrII* and *ClaI* (Figs. 2 and 3). Most of these enzymes were chosen because their sites are less likely to cluster in CpG-rich islands than sites for enzymes such as *BssHII*, *SacII*, *EagI*, etc. (Bird, 1989).

We analyzed DNA isolated from both total blood cells and the hybrid cell line CHG3, which contains human chromosome 21 in a hamster cell background. Due to differential methylation and/or RFLPs between these two sources, the results often complemented each other. For example, the *ClaI* digest of cell line CHG3 shows two fragments linking the loci S51 and S40, which do not obviously share fragments when just blood cell DNA is analyzed (Fig. 2). A *SalI* fragment present in CHG3 but not in blood DNA also links S40 and S42. Similarly, two large *NruI* fragments of  $\approx 2000$  kbp, which are present in blood cell but not in CHG3 DNA, link all loci between S42 and S25/PFKL (Fig. 3). Thus, it was important to have information from both CHG3 and blood cell DNA to construct the map. However, overall the maps from both DNA sources are very similar, indicating that the chromosome 21 region analyzed in hybrid cell line

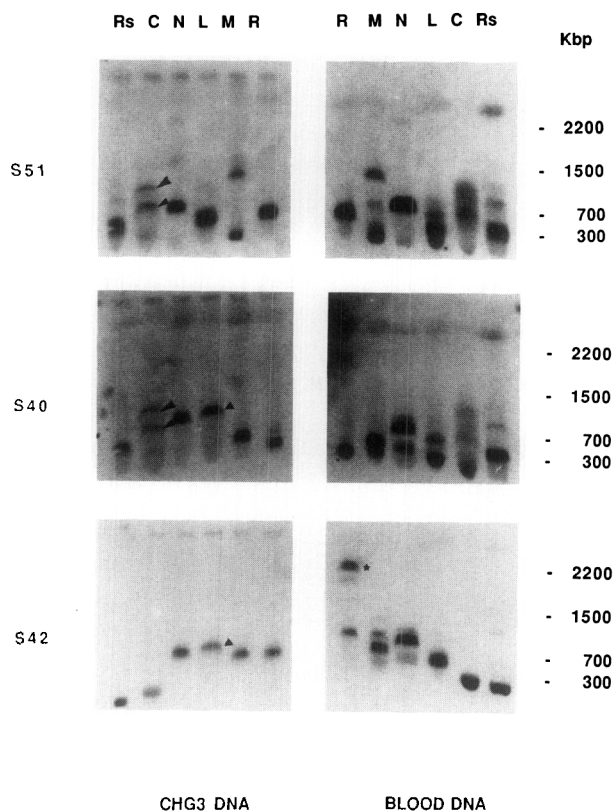


FIG. 2. PFGE comparison of DNA from the cell line CHG3 and human blood cells. One-half of a CHEF gel was loaded with restriction digests of DNA from the cell line CHG3, and the other half was loaded with DNA prepared from human peripheral blood. The migration of the DNA in the gel showed slight curvature, which was taken into account in estimating the sizes of the DNA fragments. Restriction enzymes were Rs, *RsrII*; C, *ClaI*; N, *NotI*, L, *SalI*; M, *MluI*; and R, *NruI*. CHEF gel electrophoresis was performed for 7 days at 50 V, with switching times of 20 min. The DNA from the gel was blotted onto a nylon membrane, which was hybridized successively to the probes for the loci indicated. The fragments recognized by the probe for S51 (D21S51) are very similar between the two sources, whereas the other two loci show a number of differences. The arrowheads point to fragments that were particularly useful for linking up the loci and were not present in blood DNA. The *NruI* fragments (star symbol) of about 2000 kbp are seen only in blood cell DNA and were useful for establishing a continuous map of that region (compare with Fig. 3).

CHG3, on which the RH maps are based, is not grossly rearranged.

Two DNA markers were determined to be physically linked if they recognized PFGE fragments of the same size. Figure 3 shows a total of 10 probes linked to one another on common fragments, spanning a total distance of more than 5000 kbp. In most cases, more than one DNA fragment was shared between probes, making coincidental comigration of shared fragments very unlikely. Although there is only one large (1600 kbp) *MluI* fragment in common between S3 and S101, the differential cleavage in CHG3 and blood DNA gives additional evidence that this result is not due to

coincidental comigration: for both S3 and S101, the 1600-kbp fragment hybridizes very weakly in blood cell DNA (Fig. 3), but strongly in CHG3 DNA (not shown). In addition, the two complete *MluI*-digestion products in blood cell DNA (700 and 1000 kbp) add up to the size of the partial (1600 kbp) fragment within a 10% error margin.

We were unable to obtain unequivocal evidence for physical linkage in the region near CD18. Most rare-cutting restriction enzymes cut at the same place on either side of this gene, suggesting that it is flanked by two very CpG-rich islands. Weak partial *SalI*, *RsrII*, and *ClaI* fragments suggest that CD18 is linked to its neighboring loci, S44 and S25/PFKL. Because the RH map (Fig. 1) suggests that the distance between the two flanking markers is not very large, we believe that these comigrating partial restriction fragments are probably identical rather than coincidentally of the same size. The very small fragments recognized by the two CD18 cDNA probes were also recognized by the anonymous probe for S41 (data not shown). Indeed, we found that the cDNA probes for CD18 hybridize to DNA from the phage  $\lambda$ 21, from which SF21, which recognizes the locus S41, is derived (Korenberg *et al.*, 1987). We thus established that the phage  $\lambda$ 21 contains at least part of the gene for CD18. This phage also contains sites for many rare-cutting restriction enzymes, including *NotI* and *BssHII*, and thus probably contains one of the CpG-rich islands flanking CD18.

In cases where loci were found to map very close to each other, usually within less than 800 kbp (e.g., in the S40, BCEI, S19, S49 cluster), filters were prepared from DNA fragments separated in the lower resolution range of 50–800 kbp. For this purpose, more frequently cleaving enzymes, such as *SfiI*, *BssHII*, and *EagI*, were used. Some of the data from these filters are included in Table 2. However, the orders of S141 and CRYA1, S25 and PFKL, MxA/B and S39, and BCE-I and S40, each respectively within 300 kbp of the other, could not be established. Similarly, S100B and S123 (see below) and MxA and MxB are each within 100 kbp of the other, and their order is unknown.

In summary, a physical map of the most distal region of chromosome 21 was constructed by PFGE, using a total of 24 probes. This analysis was facilitated by knowledge of the approximate positions of most markers prior to the analysis. Each marker hybridized to at least one large PFGE fragment in common with its neighbor (Table 2). This fact allowed construction of a complete, continuous map spanning about 8000 kbp (Fig. 4). Large DNA fragments of 1100–2200 kbp were most useful for linking many probes into large clusters, whereas the smaller fragments gave the order of markers within these clusters.

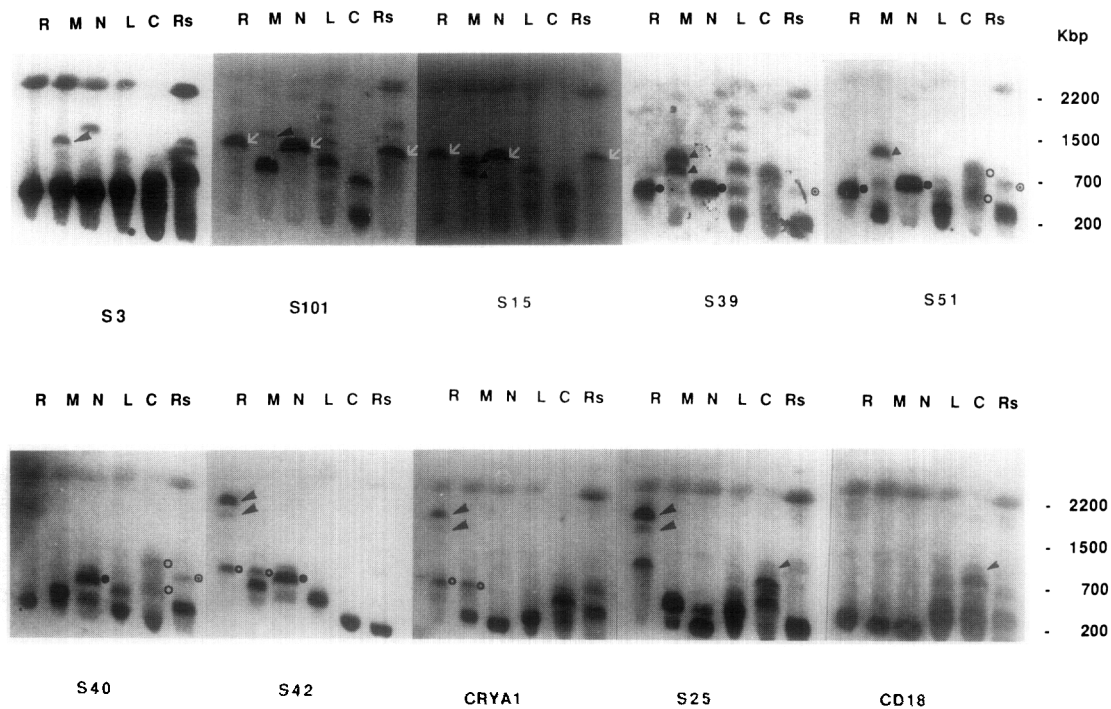


**FIG. 3.** Physical linkage of 10 loci from 21q22.3 by PFGE. The same CHEF gel described in Fig. 2, showing blood cell DNA digested with the following restriction enzymes: R, *NruI*; M, *MluI*; N, *NotI*; L, *SalI*; C, *ClaI*; Rs, *RsrII*. The gel was blotted onto a nylon membrane and was hybridized successively to probes for the loci indicated below each autoradiograph. By overlaying autoradiographs, fragments of identical size recognized by several probes were found. Identical fragments are indicated by the same symbols in successive autoradiographs. The autoradiographs are shown in the order that the loci appear in the genome, from left to right. Approximate sizes, estimated from the sizes of yeast chromosomes, are indicated in kilobase pairs (kbp) on the right.

The most informative large fragments, resulting from *MluI*, *NruI*, and *NotI* digests, are aligned in the map shown in Fig. 4.

#### Long-Range Map of the 21q Telomere

Recently, de Lange *et al.* (1990) isolated a subtelomeric DNA fragment, pTH2 $\Delta$ , that recognizes a telomere of chromosome 21, in addition to other human telomeres. Since this probe does not recognize rodent sequences, we used it for PFGE mapping on filters prepared from hybrid cell DNA containing human chromosome 21 on a mouse cell background. Figure 5 shows that several PFGE fragments are shared between this probe and the most distal markers used, S123 and S100B, which codes for the  $\beta$ -subunit of the neuronal calcium-binding protein S100 (Allore *et al.*, 1988). The smallest fragments in common among S100B, S123, and pTH2 $\Delta$  are about 200 kbp in size (see *EagI* and *SnaBI* results, Fig. 5). However, a *NaeI* fragment of  $\approx$ 50 kbp is recognized by pTH2 $\Delta$  only, placing S100B and S123 at 50 to 200 kbp from the telomere. Thus, single-copy genes and loci can be found at positions within 200 kbp of the telomere. Other genes mapping within 700 kbp of the telomere are collagen VI $\alpha$ 1 (COL6A1) and collagen VI $\alpha$ 2

(COL6A2). Both genes are within 300 kbp of each other. Their order with respect to the rest of the map was determined by a partial digest with *ClaI*, which resulted in a fragment of about 550 kbp containing both COL6A2 and S100B, but not COL6A1 (Table 2 and Fig. 5).

## DISCUSSION

#### The Map of the Telomeric 8000 kbp of Chromosome 21

We constructed a fine-structure map of the distal region of the long arm of human chromosome 21 by combining RH and PFGE mapping methods. RH mapping was not able to determine the order of loci within the two clusters S40–S49–S42 and S51–S39 due to an insufficient number of hybrids containing breaks between the loci in each cluster, whereas PFGE analysis resolved the order of markers in both cases. Conversely, PFGE did not provide unequivocal evidence for physical linkage between markers S25, CD18, and S44, whereas RH mapping indicated that these markers are closely linked. Although the RH map placed CD18 proximal to S25, the odds favoring this order over the inverted order are only 2:1. Therefore, we believe that the PFGE analysis, which placed

**TABLE 2**  
**Fragment Sizes of Markers from 21q22.3 Analyzed by PFGE**

| Locus (probe)                 | Enzyme           |                   |                  |  |                                 |                                     |   |
|-------------------------------|------------------|-------------------|------------------|--|---------------------------------|-------------------------------------|---|
|                               | <i>NotI</i>      | <i>MluI</i>       | <i>NruI</i>      | <i>SaII</i>  | <i>ClaI</i>                     | <i>RsrII</i>                        | Others  |
| S3 (pPW231)                   | 700, 1800        | 700, 1600         | 600              | 300, 800, 1700   | 250<br>600, 800, 1000           | 1200<br>1500, 1600                  |   |
| S101 (JG373)                  | 1400             | 1000, 1600        | 1400, 2000       | 300, 600, 900,<br>1100, 1500,<br>2000, 2200              | 350<br><200, 900                | 1500<br>2000                        |   |
| S15 (E8)                      | 1400             | 1250, 1400        | 1400, 2000       | 300, 600, 900,<br>1100,<br>1500, 2000, 2200              | 350<br><200, 900                | 100<br>2000                         |   |
| S39 (SF13A)                   | 700              | <200, 1250, 1400  | 600, 2000        | 500, 550, 1000<br>400, 600, 1100,<br>1500, 2000,<br>2200 | 500, 1200                       | 250, 300, 900                       |   |
| MxA/B                         | 700              | <200, 1250, 1400  | 600, 2000        | 100, <200,<br>(1000)                                     |                                 |                                     |   |
| S51 (SF93)                    | 700, (2200)      | <200, 700, 1400   | 500              | 350, 400, (1000)<br>450, 600, 750                        | 700, 1200                       | 400, 500, 1000                      |   |
| S40 (SF14)                    | (500), 900, 1000 | 500               | 250              | 250, 600, 900  | 700, 1200                       | 400, 1000                           | <i>Bss</i> III: 250                           |
| BCE-I (pS2)                   | nd               | nd                | nd               | nd, 900  | 700, 1200                       |                                     | <i>Bss</i> III: 250                           |
| S19 (B3)                      | (500), 900, 1000 | 500               | 200              | 550, 900   | 100                             | 400, 1000                           | <i>Bss</i> III: 250                           |
| S49 (SF58)                    | (500), 900, 1000 | 500               | 200              | 550, 900   | 150                             |                                     | <i>Bss</i> III: 250                           |
| S42 (SF43)                    | (500), 900, 1000 | 600, 850, (1100)  | 900, 1900, 2000  | 550, 900   | 150                             | <200, (1200)                        | <i>Bss</i> III: 100                           |
| S141 (E73)                    | 500, 1100        | <200, 850, (1100) | 900, 1900, 2000  | <200   | 900, 1100                       | 800                                 |   |
| CRYA1                         | <200             | <200, 850, (1100) | 900, 1900, 2000  | <200   | 900                             | 800                                 |   |
| S25 (p10.2)                   | <200, 400        | 700               | 1100, 1900, 2000 | 300, 600, (800),<br>(1200)                               | 300, 600, 800,<br>1100, (1500)  | <200, 500, (1400)                   |   |
| PFKL                          | <100             | 700               | ND, 1900, 2000   | 300, 600, (800),<br>(1200)                               | 300, 600, 800,<br>1100, (1500)  | nd                                  |   |
| CD18 (BLam, S41 (SF21) LAF-1) | <100             | <100              | <100             | 300, 600, (800),<br>(1200)                               | <200, 600, 800,<br>1400, (1500) | <200, 500, (1200),<br>(1400)        |   |
| S44 (SF50)                    | 400, 650, 1300   | 400               | 700              | <200, 600, 1200  | 400, 600, (1200),<br>(1500)     | 500, 550, 700,<br>(1200), (1400)    |   |
| COL6A1                        | 700, 1300        | 300               |                  | 300  | 600                             |                                     | <i>ClaI</i> partial:<br>No fragment<br>of 550 |
| COL6A2                        | 700, 1300        | 300               |                  | 300  | 250, 300                        |                                     | 550 (among<br>others)                         |
| S100B                         | 700, 1300        |                   |                  | <200   |                                 | See additional<br>results in Fig. 5 | 550 (among<br>others)                         |
| S123 (B88)                    | 700, 1300        |                   |                  |  |                                 |                                     | No fragment of<br>550                         |
| pTH2Δ                         | 700, 1300        |                   |                  |  |                                 |                                     |   |

*Note.* The approximate sizes in kbp are shown for each marker and for seven enzymes. The markers are shown in the order they appear in the genome. Nonitalicized numbers indicate fragments detected in blood cell DNA, whereas italic numbers indicate fragments seen only in DNA from the cell line CHG3. When no sizes are shown, that digest was not analyzed. Numbers indicated in parentheses correspond to faintly hybridizing fragments. Additional digests necessary to determine the order of fragments are listed in the lane marked "others." For the most telomeric region, from COL6A1 to pTH2Δ, additional information is shown in Fig. 5. The sizes were estimated from the known sizes of yeast chromosomes.

S25 proximal to CD18, provides the correct order of these markers. Similarly, although the RH map placed COL6A2 proximal to COL6A1, this order is only six times more likely than the inverted order. Because PFGE analysis provided strong evidence that places COL6A1 proximal to COL6A2, we consider this to be the correct order of these markers. With the exception of these two discrepancies, the order of loci on the RH and PFGE maps is identical. Although RH and PFGE mapping each provided inde-

pendent evidence for order and linkage of markers in this study, neither method by itself was able to produce an unequivocal map. However, in combination, the two methods were complementary and allowed the correct order of markers to be determined with greater certainty. By carrying out RH mapping prior to PFGE analysis, we were able to determine those probes that were likely to be physically close to one another. This knowledge allowed us to place probes in groups for PFGE analysis, which involves successive

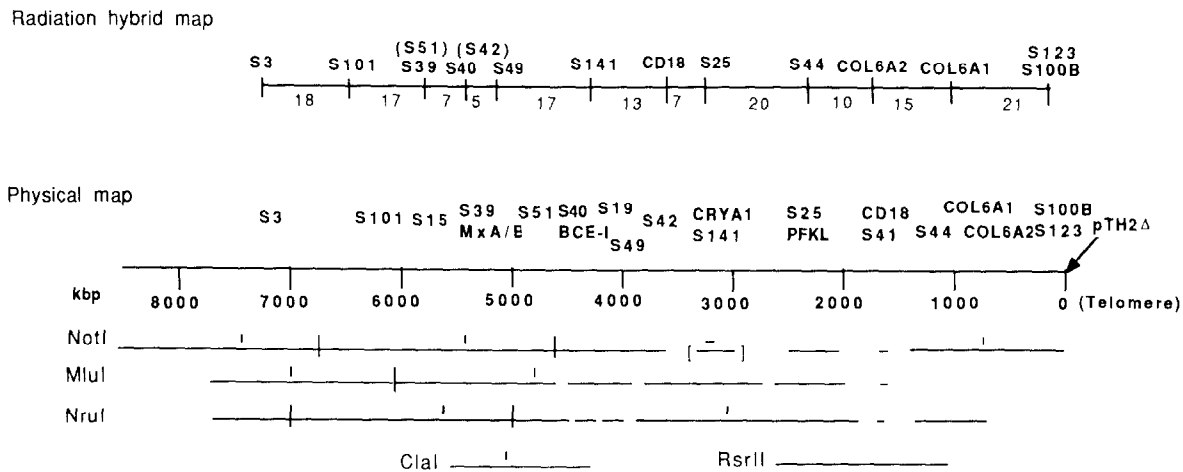


**FIG. 4.** Comparison of RH- and PFGE-derived maps of the most telomeric 8000 kbp of 21q22.3. **Top:** RH map in which the distances between the DNA markers are drawn proportional to the calculated  $cR_{8000}$  value. **Bottom:** The physical map, as determined by pulsed-field gel electrophoresis, is shown. The positions of all markers analyzed are shown above the scale. Position 0 kbp is the telomere (see also Fig. 5). Below the scale, lines indicate the most informative restriction fragments. Completely cleaved sites are indicated by vertical lines, whereas partially cleaved sites are designated by small vertical bars not touching the horizontal line. Empty spaces between horizontal lines are regions where more fragments might exist but could not be detected with the probes available. The order of the probes recognizing the two *NotI* fragments in brackets is not known. The order of the probes in the small region around position 4000 is (S40/BCE-I)–S19–S49–S42 and was determined by using additional information not shown in this figure (see Table 2). The exact physical distances around CD18/S41 are not known, but there is tentative evidence for a *RsrII* fragment of 1400–1600 kbp co-recognized by S25, CD18, and S44. Usually, the margins of the position of a marker are given by the nearest restriction sites flanking the marker (for example, S3 is between the *NotI* site at position 7400 and the *MluI/NruI* sites at position 7000).

hybridization of DNA probes to the same filter. Therefore, RH mapping improved both the speed and the efficiency of PFGE mapping.

The PFGE map spans about 8000 kbp of the telomeric region of human chromosome 21, including the telomere itself. This map was constructed with an emphasis on determining continuity and locus order rather than generating a high-resolution map (50–500 kbp) in the vicinity of each probe. In contrast to the order of markers, the sizes determined by PFGE (Table 2) may have considerable error. It is difficult to estimate fragment sizes above 1000 kbp, since there are no good size markers for this range, and pulsed-field gels separating in this size range have lower resolution. Therefore, we do not emphasize exact size determination in this study. In general, size variations of up to 20% between different studies are not uncommon. The mobility of DNA fragments depends on the PFGE system used, the amount of DNA loaded, and other unknown factors. In the Duchenne muscular dystrophy region, fragment sizes were initially overestimated considerably (Burmeister *et al.*, 1988; Den Dunnen *et al.*, 1989), and we believe that current methods still tend to overestimate rather than underestimate fragment sizes.

Gardiner *et al.* (1988, 1990) used PFGE for partial physical mapping of chromosome 21. Probes were localized into sections by using cytogenetic breakpoints, and then linked into clusters defined by comi-

grating PFGE fragments. A continuous map of the most distal region was not established, and therefore the order of markers within that region cannot be compared with our map. For probes and enzymes used in our study and in the studies of Gardiner *et al.* (1990), DNA fragment sizes agree within a 20% margin of error in the region between S3 and BCE-I (see Fig. 4). In the more distal region, several differences exist, most of which can probably be accounted for by RFLPs at rare restriction sites or by differential methylation. One striking difference, however, is the localization of the marker B88 (D21S123). It was originally reported to lie in distal 21q22.3 (Tantravahi *et al.*, 1988), which is consistent with our localization close to the telomere. Gardiner *et al.* (1990) mapped B88 to 21q22.1. However, recently, Gardiner *et al.* (K. Gardiner, personal communication) found that a different probe was used inadvertently in their studies, and they confirmed the more distal localization when the correct B88 probe was used.

#### *The Complete Map of the Long Arm*

This study, in combination with that of Cox *et al.* (1990), provides a continuous map of the long arm of human chromosome 21 with the exception of the region between the centromere and S16. The good agreement between the RH and the PFGE maps shown in this study for the distal region of the long



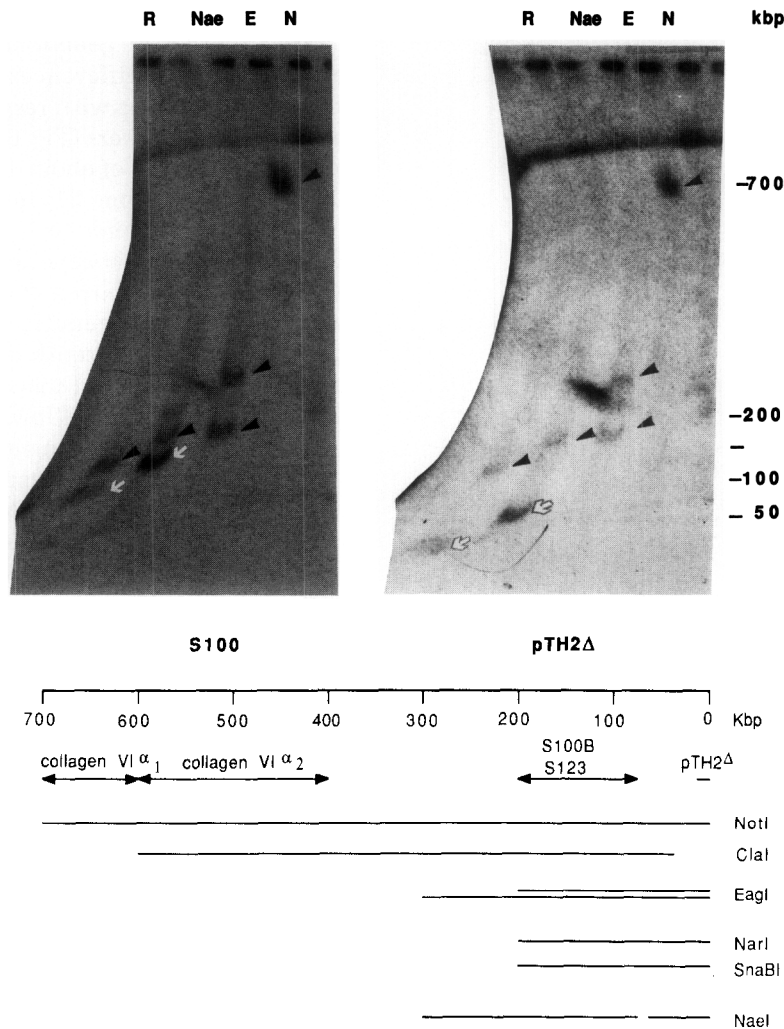


**FIG. 5.** Physical map of the 21q telomere. **Top:** PFGE analysis of the telomere. An OFAGE gel was prepared with DNA from the cell line SSC16-5, containing human chromosome 21 as the only human chromosome in a mouse background. The DNA was digested with restriction enzymes R, *Nru*I; Nae, *Nae*I; E, *Eag*I; and N, *Not*I and separated in an LKB-Pharmacia OFAGE apparatus at 280 V for 44 h with switching times of 70 s. The DNA was blotted onto nylon membranes and hybridized to the  $\beta$ -subunit of the neuronal gene S100 (S100B) and to pTH2 $\Delta$ , a probe that recognizes several human telomeres but does not recognize mouse sequences. Black arrowheads point to fragments of identical size recognized by both probes, whereas white arrowheads point to fragments of different sizes. **Bottom:** The map of the telomere as derived from the data shown above and from additional experiments. The relative order of the collagen genes was determined by hybridization of collagen VI $\alpha$ 2, S100B, and S123, but not collagen VI $\alpha$ 1 and pTH2 $\Delta$  to a 550-kbp *Cla*I fragment. The two collagen genes are less than 300 kbp apart. The order of S100B and S123 on the chromosome is not known.

arm of chromosome 21 was also observed for the proximal part of the chromosome (Cox *et al.*, 1990). Although, there was no *a priori* reason to expect that RH mapping would provide a good estimate of physical distance, data from both studies indicate that this is the case. The  $\approx 5800$  kbp between S3 and S44 are represented by 104 cR<sub>8000</sub>; thus, 1 cR<sub>8000</sub> is equivalent to 56 kbp. In the proximal region of the chromosome, 1 cR<sub>8000</sub> was found to be equivalent to about 52 kbp (Cox *et al.*, 1990). In contrast to maps of other regions of the chromosome, the RH map is expanded about twofold compared to the physical map in the telomeric  $\approx 1500$  kbp of the chromosome (see Fig. 4). Additional studies are required to determine whether

this telomeric map expansion is a general feature of RH mapping.

Given the direct relationship between RH map units and physical distance, the sizes of regions not yet covered by physical maps can now be estimated. Since 1 cR<sub>8000</sub> is equivalent to 52–56 kbp, we estimate that the region between S12 and SOD1 (83 cR<sub>8000</sub>) in the proximal half of human chromosome 21 (Cox *et al.*, 1990) spans about 4500 kbp, whereas the 113 cR<sub>8000</sub> region between SOD1 and S3 (Fig. 1) is expected to span about 6100 kbp. The total length of the long arm is thus estimated to be 35,000–39,000 kbp (assuming that the distance between S16 and the centromere is 1000–4000 kbp). This figure agrees well



chromosome 21. Here, we show that the most telomeric probes are localized on mouse chromosome 10 and extend over 2500–3000 kbp (see Fig. 4). The markers homologous to mouse chromosome 17 are more proximal on human chromosome 21. The most distal markers syntenic with mouse chromosome 16 are MxA/B (Reeves *et al.*, 1988), about 5000 kbp from the telomere (Fig. 4). Therefore, phenotypes of Down syndrome caused by genes located in the most distal 5000 kbp of chromosome 21 are not expected to be present in mice trisomic for mouse chromosome 16.

#### ACKNOWLEDGMENTS

We thank R. Allore (Toronto), M.-L. Chu (Philadelphia), J. Galt (Glasgow), Y. Groner (Rehovot, Israel), T. Kishimoto (Boston), P. Pearson (Leiden, the Netherlands), P. Staehelin (Zurich, Switzerland), G. Stewart (Ann Arbor), and P. Watkins (Framingham) for generously providing the probes used in this study, K. Frazer for developing PCR conditions for amplification of  $\alpha$ 1-crystallin, G. MacDonald for sharing material and useful discussions, and C. Pritchard, M. Hortsch, and E. Shtivelman for critically reading the manuscript. M.B. was supported by a fellowship from the gene technology program of the German Academic Exchange Committee (DAAD). This research was supported by NIH Grant HD 24610 to D.R.C. and R.M.M. T.d.L. is a Lucille P. Markey scholar, and this work was supported in part by a grant from the Lucille P. Markey foundation.

#### REFERENCES

1. AEBI, M., FAH, J., HURT, N., SAMUEL, C. E., THOMIS, D., BAZZIGHER, L., PAVLOVIC, J., HALLER, O., AND STAHEL, P. (1989). cDNA structures and regulation of two interferon-induced human Mx proteins. *Mol. Cell Biol.* **9**: 5062–5072.
2. ALLORE, R., O'HANLON, D., PRICE, R., NEILSON, K., WILKINSON, H. F., COX, D. R., MARKS, A., AND DUNN, R. J. (1988). Gene encoding the beta subunit of S100 protein is on chromosome 21: Implications for Down syndrome. *Science* **239**: 1311–1313.
3. BIRD, A. P. (1989). Two classes of observed frequency for rare-cutter sites in CpG islands. *Nucleic Acids Res.* **17**: 9485.
4. BURMEISTER, M., MONACO, A. P., GILLARD, E. F., VAN OMMEN, G. J. B., AFFARA, N. A., FERGUSON-SMITH, M. A., KUNKEL, L. M., AND LEHRACH, H. (1988). A 10-megabase physical map of human Xp21, including the Duchenne muscular dystrophy gene. *Genomics* **2**: 189–202.
- 4a. CHU, G., VOLLRATH, D., AND DAVIS, R. W. (1986). Separation of large DNA molecules by contour-clamped homogeneous electric fields. *Science* **234**: 1582–1585.
5. COX, D. R., BURMEISTER, M., PRICE, E. R., KIM, S., AND MYERS, R. M. (1990). Radiation hybrid mapping: A somatic cell genetic method for constructing high resolution maps of mammalian chromosomes. *Science* **250**: 245–250.
6. COX, D. R., PRITCHARD, C. A., UGLUM, E., CASHER, D., KOBORI, J., AND MYERS, R. M. (1989). Segregation of the Huntington disease region of human chromosome 4 in a somatic cell hybrid. *Genomics* **4**: 397–407.
7. DE LANGE, T., SHIUE, L., MYERS, R. M., COX, D. R., NAYLOR, S. L., KILLERY, A. M., AND VARMUS, H. E. (1990). The structure and variability of human chromosome ends. *Mol. Cell Biol.* **10**: 518–527.
8. DEN DUNNEN, J. T., GROOTSCHOLTEN, P. M., BAKKER, E., BLONDEN, L. A., GINJAAR, H. B., WAPENAAR, M. C., VAN PAASSEN, H. M., VAN BROECKHOVEN, C., PEARSON, P. L., AND VAN OMMEN, G. J. B. (1989). Topography of the Duchenne muscular dystrophy (DMD) gene: FIGE and cDNA analysis of 194 cases reveals 115 deletions and 13 duplications. *Amer. J. Hum. Genet.* **45**: 835–847.
9. DONIS-KELLER, H., GREEN, P., HELMS, C., CARTINHO, S., WEIFFENBACH, B., STEPHENS, K., KEITH, T. P., BOWDEN, D. W., SMITH, D. R., LANDER, E. S., *et al.* (1987). A genetic linkage map of the human genome. *Cell* **51**: 319–337.
10. FULTON, T. R., BOWCOCK, A. M., SMITH, D. R., DANESHVAR, L., GREEN, P., CAVALLI, S. L. L., AND DONIS-KELLER, H. (1989). A 12 megabase restriction map at the cystic fibrosis locus. *Nucleic Acids Res.* **17**: 271–284.
11. GALT, J., BOYD, E., CONNOR, J. M., AND FERGUSON, S. M. A. (1989). Isolation of chromosome-21-specific DNA probes and their use in the analysis of nondisjunction in Down syndrome. *Hum. Genet.* **81**: 113–119.
12. GARDINER, K., HORISBERGER, M., KRAUS, J., TANTRAVAHU, U., KORENBERG, J., RAO, V., REDDY, S., AND PATTERSON, D. (1990). Analysis of human chromosome 21: Correlation of physical and cytogenetic maps; gene and CpG island distributions. *EMBO J.* **9**: 25–34.
13. GARDINER, K., WATKINS, P., MÜNKE, M., DRABKIN, H., JONES, C., AND PATTERSON, D. (1988). Partial physical map of human chromosome 21. *Somat. Cell Mol. Genet.* **14**: 623–637.
14. HERRMANN, B. G., BARLOW, D. P., AND LEHRACH, H. (1987). A large inverted duplication allows homologous recombination between chromosomes heterozygous for the proximal t complex inversion. *Cell* **48**: 813–825.
15. JACKSON, J. F., NORTH, E. R., AND THOMAS, J. G. (1976). Clinical diagnosis of Down's syndrome. *Clin. Genet.* **9**: 483–487.
16. KISHIMOTO, T. K., O'CONNOR, K., LEE, A., ROBERTS, T. M., AND SPRINGER, T. A. (1987). Cloning of the beta subunit of the leukocyte adhesion proteins: Homology to an extracellular matrix receptor defines a novel supergene family. *Cell* **48**: 681–690.
17. KORENBERG, J. R., CROYLE, M. L., AND COX, D. R. (1987). Isolation and regional mapping of DNA sequences unique to human chromosome 21. *Amer. J. Hum. Genet.* **41**: 963–978.
18. LAURIE, D. A., AND HULTEN, M. A. (1985). Further studies on chiasma distribution and interference in the human male. *Ann. Hum. Genet.* **49**: 203–214.
19. LEVANON, D., DANCIGER, E., DAFNI, N., AND GRONER, Y. (1987). Construction of a cDNA clone containing the entire coding region of the human liver-type phosphofructokinase. *Biochem. Biophys. Res. Commun.* **147**: 1182–1187.
20. LIEMAN-HURWITZ, J., DAFNI, N., LAVIE, V., AND GRONER, Y. (1982). Human cytoplasmic superoxide dismutase cDNA clone: A probe for studying the molecular biology of Down syndrome. *Proc. Natl. Acad. Sci. USA* **79**: 2808–2811.
21. MACDONALD, G. P., PRICE, E. R., CHU, M.-L., TIMPL, R., ALLORE, R., MARKS, A., DUNN, R., AND COX, D. R. (1988). Assignment of four human chromosome 21 genes to mouse chromosome 10: Implications for mouse models of Down syndrome. *Amer. J. Hum. Genet. Suppl.* **43**: A151 (Abstract).
22. MCCORMICK, M. K., SCHINZEL, A., PETERSEN, M. B., STETTEN, G., DRISCOLL, D. J., CANTU, E. S., TRANEBAERG, L., MIKKELSEN, M., WATKINS, P. C., AND ANTONARAKIS, S. E. (1989). Molecular genetic approach to the characterization of

- the "Down syndrome region" of chromosome 21. *Genomics* **5**: 325-331.
23. McDEVITT, D. S., HAWKINS, J. W., JAWORSKI, C. J., AND PIATIGORSKY, J. (1986). Isolation and partial characterization of the human alpha A-crystallin gene. *Exp. Eye Res.* **43**: 285-291.
  24. MILLINGTON, W. A. M., AND PEARSON, P. L. (1988). Use of restriction fragment length polymorphic probes in the analysis of Down's syndrome trisomy. *Hum. Genet.* **80**: 362-370.
  25. MOISAN, J. P., MATTEI, M. G., AND MANDEL, J. L. (1988). Chromosome localization and polymorphism of an oestrogen-inducible gene specifically expressed in some breast cancers. *Hum. Genet.* **79**: 168-171.
  26. MÜNKE, M., KRAUS, J. P., OHURA, T., AND FRANCKE, U. (1988). The gene for cystathionine beta-synthase (CBS) maps to the subtelomeric region on human chromosome 21q and to proximal mouse chromosome 17. *Amer. J. Hum. Genet.* **42**: 550-559.
  27. PATTERSON, D., VAN KEUREN, M., DRABKIN, H., WATKINS, P., GUSELLA, J., AND SCOGGIN, C. (1985). Molecular analysis of chromosome 21 using somatic cell hybrids. *Ann. N. Y. Acad. Sci.* **450**: 109-120.
  28. PETERSEN, M. B., SLAUGENHAUPT, S. A., LEWIS, J. G., WARREN, A. C., CHAKRAVARTI, A., AND ANTONARAKIS, S. E. (1989). A genetic linkage map of 24 loci on human chromosome 21. *Amer. J. Hum. Genet. Suppl.* **45**: A157 (Abstract).
  29. PRITCHARD, C. A., CASHER, D., UGLUM, E., COX, D. R., AND MYERS, R. M. (1989). Isolation and field-inversion gel electrophoresis analysis of DNA markers located close to the Huntington disease gene. *Genomics* **4**: 408-418.
  30. RAHMANI, Z., BLOUIN, J. L., CREAU, G. N., WATKINS, P. C., MATTEI, J. F., POISSONNIER, M., PRIEUR, M., CHETTOUH, Z., NICOLE, A., AURIAS, A., *et al.* (1989). Critical role of the D21S55 region on chromosome 21 in the pathogenesis of Down syndrome. *Proc. Natl. Acad. Sci. USA* **86**: 5958-5962.
  31. REEVES, R. H., O'HARA, B. F., PAVAN, W. J., GEARHART, J. D., AND HALLER, O. (1988). Genetic mapping of the Mx influenza virus resistance gene within the region of mouse chromosome 16 that is homologous to human chromosome 21. *J. Virol.* **62**: 4372-4375.
  32. REEVES, R. H., ROBAKIS, N. K., OSTER, G. M. L., WISNIEWSKI, H. M., COYLE, J. T., AND GEARHART, J. D. (1987). Genetic linkage in the mouse of genes involved in Down syndrome and Alzheimer's disease in man. *Brain Res.* **388**: 215-221.
  33. SAIKI, R. K., GELFAND, D. H., STOFFEL, S., SCHARF, S. J., HIGUCHI, R., HORN, G. T., MULLIS, K. B., AND ERLICH, H. A. (1988). Primer-directed enzymatic amplification of DNA with a thermostable DNA polymerase. *Science* **239**: 487-491.
  34. SCHWARTZ, D. C., AND CANTOR, C. R. (1984). Separation of yeast chromosome-sized DNAs by pulsed field gradient gel electrophoresis. *Cell* **37**: 67-75.
  35. SKOW, L. C., AND DONNER, M. E. (1985). The locus encoding alpha A-crystallin is closely linked to H-2K on mouse chromosome 17. *Genetics* **110**: 723-732.
  36. STEWART, G. D., HARRIS, P., GALT, J., AND FERGUSON, S. M. A. (1985). Cloned DNA probes regionally mapped to human chromosome 21 and their use in determining the origin of nondisjunction. *Nucleic Acids Res.* **13**: 4125-4132.
  37. TANTRAVAHU, U., STEWART, G. D., VAN KEUREN, M., MCNEIL, G., ROY, S., PATTERSON, D., DRABKIN, H., LANDE, M., KURNIT, D. M., AND LATT, S. A. (1988). Isolation of DNA sequences on human chromosome 21 by application of a recombination-based assay to DNA from flow-sorted chromosomes. *Hum. Genet.* **79**: 196-202.
  38. TANZI, R. E., HAINES, J. L., WATKINS, P. C., STEWART, G. D., WALLACE, M. R., HALLEWELL, R., WONG, C., WEXLER, N. S., CONNEALLY, P. M., AND GUSELLA, J. F. (1988). Genetic linkage map of human chromosome 21. *Genomics* **3**: 129-136.
  39. VAN DYKE, D. L., WORSHAM, M. J., FISHER, L. J., AND WEISS, L. (1986). The centromere index and relative length of human high-resolution G-banded chromosomes. *Hum. Genet.* **73**: 130-132.
  40. WARREN, A. C., SLAUGENHAUPT, S. A., LEWIS, J. G., CHAKRAVARTI, A., AND ANTONARAKIS, S. E. (1989). A genetic linkage map of 17 markers on human chromosome 21. *Genomics* **4**: 579-591.
  41. WATKINS, P. C., TANZI, R. E., GIBBONS, K. T., TRICOLI, J. V., LANDES, G., EDDY, R., SHOWS, T. B., AND GUSELLA, J. F. (1985). Isolation of polymorphic DNA segments from human chromosome 21. *Nucleic Acids Res.* **13**: 6075-6088.
  42. WEIL, D., MATTEI, M. G., PASSAGE, E., NGUYEN, V. C., PRIBULA, C. D., MANN, K., DEUTZMANN, R., TIMPL, R., AND CHU, M. L. (1988). Cloning and chromosomal localization of human genes encoding the three chains of type VI collagen. *Amer. J. Hum. Genet.* **42**: 435-445.